Scalable Minimally Actuated Leg Extension Bipedal Walker Based on 3D Passive Dynamics

Sharfin Islam*[1,2], Kamal Carter*[1], Justin Yim*[1], James Kyle[1], Sarah Bergbreiter[1], and Aaron M. Johnson[1]

***Abstract*— We present simplified 2D dynamic models of the 3D, passive dynamic inspired walking gait of a physical quasi-passive walking robot. Quasi-passive walkers are robots that integrate passive walking principles and some form of actuation. Our ultimate goal is to better understand the dynamics of actuated walking in order to create miniature, untethered, bipedal walking robots. At these smaller scales there is limited space and power available, and so in this work we leverage the passive dynamics of walking to reduce the burden on the actuators and controllers. Prior quasi-passive walkers are much larger than our intended scale, have more complicated mechanical designs, and require more precise feedback control and/or learning algorithms. By leveraging the passive 3D dynamics, carefully designing the spherical feet, and changing the actuation scheme, we are able to produce a very simple 3D bipedal walking model that has a total of 5 rigid bodies and a single actuator per leg. Additionally, the model requires no feedback as each actuator is controlled by an open-loop sinusoidal profile. We validate this model in 2D simulations in which we measure the stability properties while varying the leg length/amplitude ratio, the frequency of actuation, and the spherical foot profile. These results are also validated experimentally on a 3D walking robot (15cm leg length) that implements the modeled walking dynamics. Finally, we experimentally investigate the ability to control the heading of the robot by changing the open-loop control parameters of the robot.**

I. Introduction

Small robots have the potential to traverse confined areas and give us an entirely new subset of environments to navigate [1]. Among others, magnetic hexapod [2], micro bristle walkers [3], and piezoelectric actuated hexapods [4] have shown the potential of small legged robots, but less attention has been given to bipedal walkers. Small bipedal robots share the same potential of navigating small spaces with a simpler body, and also could be used in film, toys, and other entertainment industries.

Bipedal robots present a unique problem in the need for both stability and motion control [5]. Shrinking a bipedal walker means there is limited room for actuation, control, and sensing to accomplish both these tasks. Fortunately, passive dynamic walking presents a method to reduce the design and control complexity. Our goal is to leverage passive dynamics to create a minimally actuated and controlled bipedal walking model that can be shrunk to a centimeter-scale.

* Equal Contributors. This work was supported in part by the National Science Foundation under Grants IIS-1813920 and CCF-2030859 to the Computing Research Association for the CIFellows Project.

[1]Department of Mechanical Engineering, Carnegie Mellon University, Pittsburgh, PA 15213, USA, amj1@cmu.edu

[2]Department of Mechanical Engineering, Columbia University, New York, NY 10027, USA

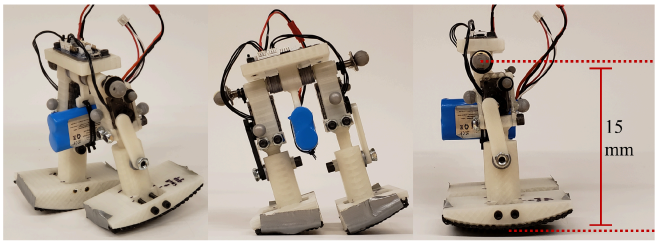

Fig. 1. A small (15cm leg length), minimally actuated, quasi-passive walker capable of walking and turning with open-loop control and a single actuator per leg. The nonconcentric foot curvature, hip position, and mass distribution are key to stable walking.

There has been substantial work done in bipedal walkers with minimally complex designs and control schemes. Dating back to 1990, Tad McGeer introduced the concept of passive dynamic walking [6], inspired by walking toys [7]. McGeer was able to develop a walking model that could maintain a stable gait down a slope without any actuation or control. The walking model integrated curved, spherical feet to allow the walker to roll laterally and pitch forward. These aspects of passive walking have been integrated with actuators to open a new field of quasi-passive walkers [8–14].

In this paper we integrate the principles of passive dynamic walking into a scalable active bipedal walking model with a very simple design and control scheme. Nondimensionalizing rigid body mechanics with Coulombic friction allows insights at larger sizes to be easily scaled to smaller platforms. Similar to other quasi passive walking models, e.g [6,8], we separate the frontal and sagittal plane to approximate the 3D dynamics. We then use these 2D models to derive design constraints and build a small (15cm leg length) 3D bipedal walking robot, Fig. 1.

In addition to maintaining a stable gait on flat ground, our walker has several features that make it unique compared to prior work: 1) it does not require exact initial conditions, and can self-start from a standing posture, 2) it has a wide range of parameters in which the walker can maintain a stable gait, 3) it shows the potential to control the yaw without actuation of that specific degree of freedom, and 4) it has a very simple design and control. One of the key elements to enable success in this model and robot is the nonconcentric spherical feet, and we show that this foot design produces stable walking at a wide range of control amplitudes and frequencies.

The rest of the paper is organized as follows. The remainder of this section summarizes the related work on quasi-passive walking models (Sec. I-A) and robots (Sec. I-B). Then, Sec. II presents the walking model, including the control strategy and constraints on the model design. Sec. III

details both the simulation and physical robot experimental setups. Sec. IV shows results establishing the robustness of the walking to control parameters, the importance of the foot design, and the steering abilities. Finally, Sec. V discusses some conclusions and future directions.

A. Walking Models

From humans to passive walkers, several walking models have been established for different gaits. McGeer established the sagittal plane walking model for passive dynamic walkers with curved feet on slopes [6]. This model can be further simplified to have point feet as a compass gait model [15,16]. For quasi-passive walkers, sagittal plane compass models integrate leg extension actuators with point [17] or curved [18] feet. Other actuation schemes include hip actuation and toe-off impulse [14,19,20].

In the frontal plane, the basic model of passive walking draws from an analogy to a wobbling domino [21]. These walkers often use spherical feet sharing a common center of curvature, such as in [8,11,13]. In [22], the feet uniquely have independent centers of rotations similar to our model.

To implement these models in physical walkers, the frontal and sagittal plane models must be coupled to ensure the full system walks correctly [22,23]. The 3D quasi-passive walkers mentioned above all simplify the 3D walking into 2D walking models. Coupling the frontal and sagittal plane is difficult and creates many issues. For example, many passive walkers have had trouble in compensating for unwanted yaw oscillation [8,24]. Modified frontal plane models using statically equivalent flat foot spring feet have been developed to solve this issue [11,13,25].

Our model presents unique benefits from those discussed above, especially for smaller scales. Specifically, leg extension is easily scalable as there are a myriad of small linear MEMS actuators and linear motion can realized in several ways [26]. The nonconcentric spherical feet turn out to be key to the robustness of our model. We are also able to control the yaw of our robot without a more complicated flat-foot spring design. Finally, we successfully couple the frontal and sagittal planes without the need of a feedback controller with a passive hip using only a forward hip offset. Our 2D planar models are detailed in Section II and our experimental results are shown in Section IV.

B. Quasi-Passive Walkers

McGeer's walker was able to walk without actuation because it was set on a slight decline, therefore leveraging gravity to swing the legs forward [6]. Putting a walker on flat ground, actuation is needed to inject energy and recover the losses from foot impact. Several robots have used unique actuation and control schemes to leverage passive dynamics.

For example, the Cornell Ranger leverages curved feet to achieve an energy-efficient gait with an actuated hip and ankle at each leg [10]. Other robots use ankle actuators to roll and pitch the robot forward, like the MIT Toddler [8]. This walker had curved, spherical feet like those in McGeer's original passive dynamic walker. Through the foot geometry and actuation strategy, the MIT walker was able to maintain a stable 3D walk on flat ground. Similarly, the RW04 mimicked spherical feet to create a minimally actuated 3D walker with a passive hip [11]. RW04 used flat feet with a combination of springs to mimic the forces of curved feet. The TENBU [13], similar to RW04, created a statically equivalent flat foot that leveraged springs to mimic the oscillatory behavior of McGeer's spherical feet. TENBU, however, uses pneumatic artificial muscles to roll and pitch, while RW04 only uses actuators to wobble side-to-side for leg clearance to swing the leg forward. A mechanical oscillator can also be used to inject energy and achieve a 3D passive walking gait, e.g. as shown in simulation in [12].

TABLE I
COMPARISON OF DIFFERENT PASSIVE DYNAMICS INSPIRED WALKERS.

	Cornell	Meta	MIT	RW04	Ours
Citation	[10]	[9]	[8]	[11]	-
Mass (kg)	12.7	8.0	2.9	6.5	0.365
Leg Length (m)	0.81	1.255	0.44	0.807	0.15
Actuated DOF	3	2	4	2	2
Capable of open loop walking?	No	No	Yes	Yes	Yes

Several of these walkers use feedback control to ensure stable gaits, including velocity control [8], reflex-based control [9,10], zero moment point trajectory control [11], and position based control used to coordinate different joints [14]. These sensory feedback methods often serve to resolve the issues in coupling the 2D dynamic models into a 3D walking gait. However, open loop controllers have worked in minimally actuated walkers such as RW04 [11] and the MIT Toddler [8]. However, RW04 saw large bands of frequencies in which their sinusoidal controller did not work and the Toddler had difficulty stabilizing roll oscillations when the robot started out of phase. Both these walkers noted the need for sensory feedback for a more robust and stable gait.

Despite the diverse actuation and designs of the walkers mentioned, all share similarities in leveraging passive dynamics and minimal actuation to produce stable gaits.

In Table I, we compare some of these robots to our physical walker. Our robot is simpler in terms of mass, size, mechanical complexity, and control. This makes it easier to build and also means that it is easier to scale our walker down to even smaller sizes. Additionally, as these walkers were not meant to be scaled, the MIT and RW04 have several additional mechanical components such as springs, ball screws, and several rigid bodies that would be difficult to include at smaller sizes.

II. MODEL OF QUASI-PASSIVE WALKER

Our walking model, shown in Fig. 2, consists of 5 rigid bodies – a torso, two upper legs, and two spherical section feet. The hip joint is passive, but there is an actuated prismatic joint in each of the two leg.

As mentioned in Sec. I-B, we simplify the 3D dynamics into frontal and sagittal planes. In these planar models the torso rigid body is neglected and its mass is lumped into the upper legs. The system follows Lagrangian rigid-body dynamics with model parameters listed in Table II. In both

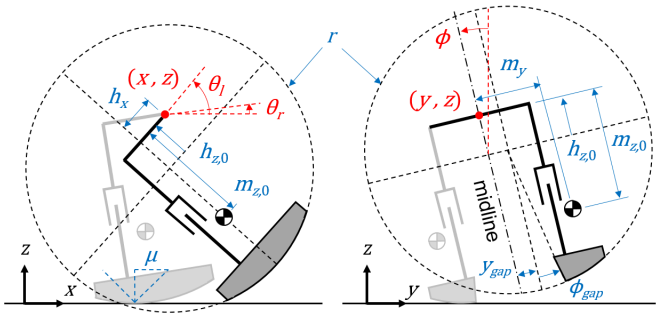

Fig. 2. The robot's generalized coordinates (red) and kinematic parameters (blue) in a simplified model for both sagittal (left) and frontal (right) planes.

TABLE II

PARAMETERS FOR THE MODEL FOUND IN FIG. 2.

Parameter	Description	Physical Value
r	Radius of curvature	15.2 cm
y_{gap}	Distance between feets' centers of curvature	0.1 cm or 0.9cm
ϕ_{gap}	Angle of foot interior edges	0 or -0.136 rad
$h_x, h_{z,0}$	Nominal hip displacement from foot center of curvature	0.8 cm, -1.1cm
$m_y, m_{z,0}$	Nominal displacement of each leg's center of gravity (CG) from the center of the hip	2 cm, 8.1 cm
$I_{leg,xx}$, $I_{leg,yy}$	Moment of inertia of each leg	both 6 kg*cm^2
m	Mass of each leg	136 g
μ	Coefficient of friction	0.5

planar simulations, the generalized coordinates are the Cartesian coordinates of the center of the hip axle, the angles of the legs (θ_l, θ_r in the sagittal, and ϕ in the frontal plane), and the two leg lengths. Linear actuation is modelled as stiff position control, simplifying each leg's pair of rigid bodies into a single rigid body with length varying with amplitude A about the nominal value $h_{z,0} + r$ and and center of gravity (CG) height m_z varying with $\frac{1}{5}A$ (the lower leg mass fraction). The moments of inertia are assumed constant since $2A$ is less than 10% of the leg length. In the stance phase, the feet make rolling contact with the ground (with or without sliding) with Coulombic static and dynamic coefficients of friction of 0.5. Touchdown transitions are modeled as inelastic impacts. While we did not model the coupling between the two planar models, their footfall timings agree with each other and with experimental results during the stable gaits of interest.

The stability of the walking behavior requires several constraints on the parameters of the design, as summarized in Table III. First, the center of gravity must be below the center of curvature for static stability. This rule has been well established in passive dynamic models since [21]. ϕ_{gap} and y_{gap} both relate to the foot shape, and these constraints are further explored in Fig. 3 and Sec. IV. The constraints on h_x and m_z ensure the legs swing forward when they gain ground clearance. Without these constraints, the walker will not move forward. RW04 implements a similar offset, but by moving the center of mass and keeping the hip in line with the legs [11].

A key aspect of the model is the foot shape. As mentioned

TABLE III

DESIGN RULES FOR STABLE WALKING.

Design Rule	Description
$-h_z + m_z > 0$	Center of gravity (CG) below radius of curvature for static stability
$y_{gap} > 0$	Positive separation between feet centers of curvature
$\phi_{gap} \leq 0$	Foot rests of curved surface when standing upright
$h_x > 0$	Forwards hip offset initiates forwards walking
$m_z > 0$	Center of gravity (CG) below hip so that the leg hangs downwards in swing

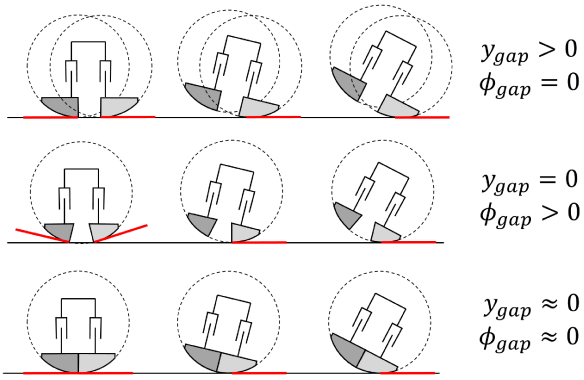

Fig. 3. Different foot geometries used in simulation and experiments. Top row: Nonconcentric feet with a gap. Middle row: Concentric feet with a gap. Bottom row: Feet with a negligible gap. Red lines indicate the contact point and angle of the surface of the foot at the contact point.

above, passive models usually have concentric spherical feet. Each foot in our model has two parameters related to lateral spacing, ϕ_{gap} and y_{gap}, similar to [22]. Our simulation and experimental testing in Sec. IV show that these two parameters are important to the stability of the walker.

A gap between the feet can be produced with a positive y_{gap} or ϕ_{gap} and removed by setting both to 0, creating three cases shown in Fig. 3. In the first case, we evaluated a walker in which $y_{gap} = 0.9$ cm and the spheres defining the feet are not concentric. In the second case, there is a gap ($\phi_{gap} = 3.4°$) and the spheres defining the foot profiles are concentric. In this concentric case, there is the possibility of a sharp transition in which the feet are no longer tangent to the ground at impact due to the foot profile and gap angle. In the last case, there is a negligible foot gap ($y_{gap} = 0.1$ cm) and the feet are considered concentric. All other parameters were the same throughout these three trials.

Finally, one useful property of the model is that it scales isometrically [27]. This is a key benefit as it allows for reasoning about larger and smaller walking machines. However, the model does not consider friction and damping in the joints, the stiffness of the rigid bodies, or surface effects that may change as we move to smaller scales.

A. Open-loop Sinusoidal Control

The walking model does not require any feedback sensing for control. Each leg is controlled by a sinusoidal trajectory with an amplitude A, nominal length $h_{z,0}+r$, and frequency

ω offset by 180° between the two legs as follows,

$$l_r^d = (h_{z,0} + r) + A\sin(\omega t) \quad (1)$$

$$l_l^d = (h_{z,0} + r) + A\sin(\omega t + 180°) \quad (2)$$

To turn while walking, we modify the phase offset in (2) to be less than 180° for turning left and greater than 180° for turning right.

This actuation scheme results in the stance leg extended past nominal during the stance phase and retracted during the swing phase. During double stance, with a phase offset of 180°, both legs are at the nominal length. The stance leg extending and the swing leg retracting allow for increased swing leg clearance. Note that unlike walkers that inject energy by extending the leg at the transition out of stance, energy injection in this model occurs during the continuous stance phase. This open loop control method also emphasizes some other previously held notions about quasi-passive walkers as well. Specifically, other walkers that implement prismatic leg joints have shown that the exact trajectory of the legs does not matter as long as energy that is lost is re-injected by the actuators [11,20,28]. Therefore, our walker does not require feedback for a simple walking gait. As shown in Sec. IV, this open-loop control algorithm achieves this goal at a variety of different amplitudes and frequencies for multiple foot configurations.

III. Experimental and Simulation Set-up

A. Simulation Methods

From the dynamic model defined in Sec. II, we developed two independent planar simulations for the sagittal and frontal planes implemented in MATLAB using `ode45` with event finding [29].

The simulation was evaluated by three metrics which include: 1) sagittal plane walking speed, 2) roll bias (the magnitude of any steady left or right lean), and 3) consistency (the standard deviation (STD) of the timing of the left leg touchdown relative to the phase of the sinusoidal leg actuation). We varied the foot geometry y_{gap} and ϕ_{gap}, actuation amplitude A, and actuation frequency ω. The remaining parameters used in the simulation match those of our physical walker, as listed in Table II.

B. Prototype Assembly and Fabrication

The walker shown in Fig. 1 follows the dimensions listed in Table II. The walker is primarily 3D printed out of PLA, with a simple rubber non-slip shelf liner taped to the bottom of each foot to increase friction (any high-friction material to limit slipping will work). The assembly is comprised of a torso, a 1/4" aluminum rod with plastic bushings for the hip joint, two legs, and two feet. Each leg is assembled from a Dynamixel XL-320 servo, a two part housing for the servo, and a two-part crank-link mechanism in which the servo extends or retracts the foot. As our connecting rod is much longer than our crank, this linkage approximates the profiles seen in (1) and (2). The torso houses the OpenCM9.04 controller on the top and a 7.4V lithium ion battery which hangs below the hip joint. Each foot attaches to the leg on a bolt which can be tightened to narrow the gap, allowing quick change of the feet between the first and third geometries shown in Fig. 3 or replacement of the feet with another set with nonzero ϕ_{gap}.

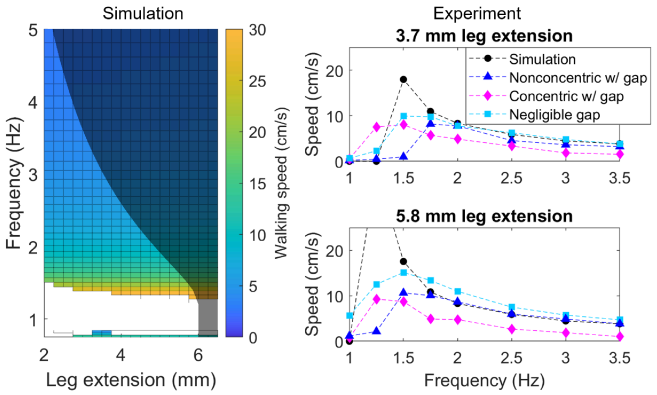

Fig. 4. Forward walking speed simulation (left) and experimental (right) results from sagittal plane model at different frequencies and amplitudes of oscillations. For the simulation: White region is unsuccessful walking and the dark region indicates the actuation limit of the servo used on the physical robot. Experimental trends follow simulation predictions: the highest walking speed is achieved between 1.25 and 1.5 Hz, and the speed gradually decreases with increasing frequency above that point.

In the assembled robot, we found that tight joints, especially at the connection of the two-part servo housing, are necessary for the legs to perform as intended in the model. Slight movement in this joint in particular caused the leg to bow inwards effectively changing the intended foot gap. Additionally, friction reduction at the two-part sliding leg joint was important in reducing sticking upon extension and retraction. Sanding of the inner component of the two-part sliding leg joint and a small gap between the crank and the bottom leg component are both used to reduce friction and stiction. The small servo's maximum speed limited the amplitude of leg extension at high frequencies, shown as a dark region in Figs. 4 and 7.

Experimental data were collected using an Optitrack motion capture system running at 100 Hz. The spatial position and orientation of each upper leg was tracked. To mitigate tracking noise, we filtered the data with a 5-point moving median filter followed by a 3-point moving average filter. The walker is allowed to converge for 10 strides (20 steps) and the following 15 strides are used for evaluation.

IV. Results

A. Sagittal Plane Simulation and Testing

To measure the forward speed and walking stability, we tested a range of parameters in the sagittal plane simulation, with the results shown in Fig. 4. Note that there is only one plot for the pitch simulations despite the three configurations shown in Fig. 3 – this is because y_{gap}, ϕ_{gap}, and the frontal foot profile do not appear in the sagittal plane model.

There are three features to note in these simulation results. First, there is a negative correlation between the frequency and walking speed. As the frequency of leg extension increases for any given amplitude, the walker moves slower.

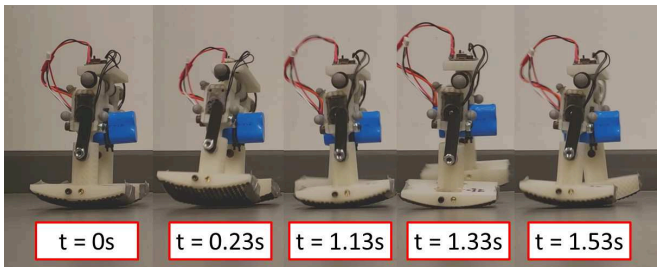

Fig. 5. Our walker moving forward (rightward) with passive dynamic inspired feet, a forward hip offset for forward leg swing, and a single leg extension actuator per leg driven by an open loop sinusoidal control signal

Secondly, there is a minimum frequency for the model to successfully walk forward, indicated by the white region in Fig. 4. The walker is self starting and enough energy needs to be injected by the prismatic joints for the legs to gain initial clearance off the ground. Finally, there is a small strip of "valid" solutions around $\omega = 0.75$ Hz and starting from $A = 2.5$ mm. These are not physically possible since the roll would not allow the legs to swing forward. This highlights the fact that our simulation does not include any coupling between the pitch and roll modes, which is important to understand non-physical simulation results such as these.

Forward walking tests on the robot, an example of which is shown in Fig. 5, follow similar trends as the simulation results. These trials were self-starting from a standing posture and reached a maximum speed of 140 mm/s, or about one leg length per second. We show the results for different frequencies, amplitudes, and foot geometries in Fig. 4. We see a negative relationship between velocity and frequency, following our simulation results.

The robot was unable to make forward progress at low frequencies both in simulation and experiment, but the simulation predicted a minimum frequency for walking that was slightly too low and corresponded to a very high peak forward walking speed not seen in physical experiment. The simulation was most accurate for the nonconentric gap case. The median absolute error in velocity was 0.69 cm/s for the nonconcentric gap case, 1.46 cm/s for the negligible gap case, and 3.34 cm/s for the concentric gap case.

B. Frontal Plane Simulation and Testing

For frontal plane simulation and testing, each combination of frequency and amplitude was evaluated by its consistency and roll bias into three categories: good walking, leaning, and inconsistent, as shown in Table IV. Thresholds for these categories were determined by observing the qualitative convergence and turning of the experimental and simulated trajectories. Example roll and pitch data collected from motion capture experiments are shown in Fig. 6. In experiments, heel strike is detected when the pitch velocity reverses from positive to negative. Full parameter sweeps are given in Fig. 7 for simulation and experiments on all three foot geometries.

Most spherical feet in quasi-passive walkers are concentric with a non-negligible gap. However, our walking model behaved more consistently both in simulation and in physical testing with non-concentric feet. In Table V, we see that the

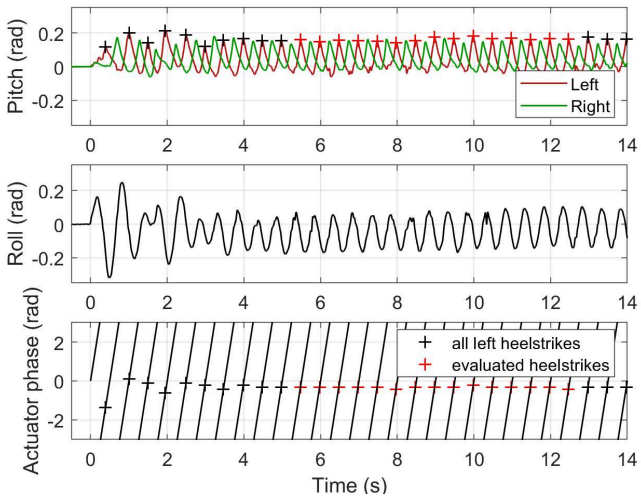

Fig. 6. Example experimental data for nonconcentric gap feet, 5.8mm amplitude, and 2 Hz frequency test. Top - Pitch of left and right feet with marks indicating heel strike. Middle - Body roll. Bottom - Actuator phase and heel strike (calculated by sinusoidal trajectory, (1) and (2)).

TABLE IV
ROLL CONSISTENCY CATEGORIZATION FOR SIMULATION TESTING.

Fig. 7 Color	Categorization	Condition
	Good Walking	STD $<$ 0.1 rad, bias $<$ 0.09 rad
	Leaning	STD $<$ 0.1 rad, bias $>$ 0.09 rad
	Inconsistent	STD $>$ 0.1

nonconcentric feet had the lowest median actuator STD for both simulation and experimental results. While the walker made forward progress in most trials in which it lifted its feet (those outside the white region of Fig. 4), inconsistency and bias in the gait tend to make the robot veer left or right.

There is a large region of consistent behavior for nonconcentric feet with a gap. As shown in Fig. 7, nonconcentric feet have the most "good walking" trials in both simulation and experiment and this region of good walking is contiguous, allowing for a significant range of parameter variation.

The simulation and experimental results match best for the nonconcentric gap, as shown in Table V. The discrepancy between simulation and experiments in the concentric gap is due to the much more consistent walking in experiments at low amplitudes, possibly a result of unmodeled flexing or 3D coupling in testing that is not captured in our 2D simulation. Similarly, the poor performance of the concentric no gap case might be affected by the limitations of our simulation. The concentric feet with no gap never achieved consistency better than 0.1 rad using the smaller 3.8 mm amplitude extension, but at 1.5 and 1.75 Hz it had a consistency of 0.18 rad and made steady and straight forward progress. Anecdotally, the concentric foot walkers performed better with more inefficiencies (such as loose fasteners) that dissipated energy due to non-rigid attachment points.

Despite not matching our simulation, it is promising to see there are a number of good walking trials for concentric feet with a gap. The success of both configurations with a gap might indicate a possible relationship between stability and gap width.

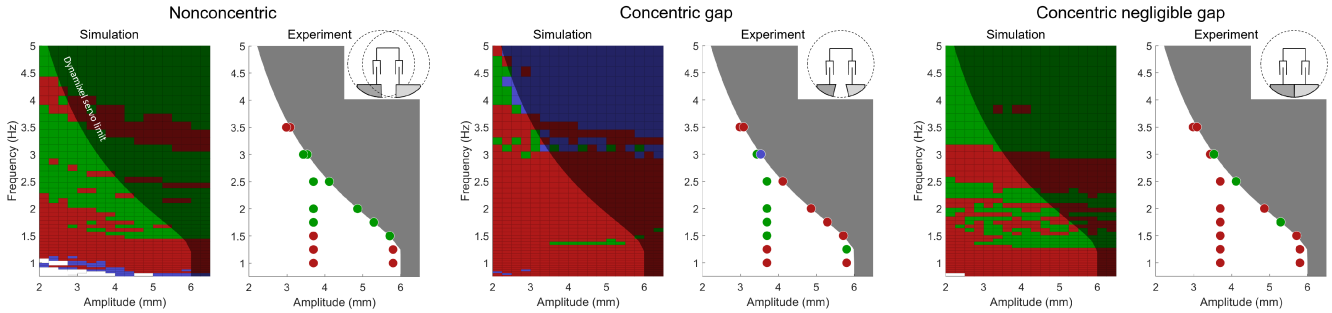

Fig. 7. Roll consistency results from simulation and experiment for each of the configurations shown in Figure 3. Good walking (green), leaning (blue), and inconsistent (red) categorization are defined in Table IV.

TABLE V

MEDIAN SIMULATION AND EXPERIMENTAL ROLL CONSISTENCY FOR EACH OF THE CONFIGURATIONS SHOWN IN FIG. 7.

	Median Actuator STD (rad)	
	Simulation	**Experimental**
Nonconcentric	0.1318	0.1424
Concentric Gap	0.4739	0.1524
Negligible Gap	0.2506	0.2641

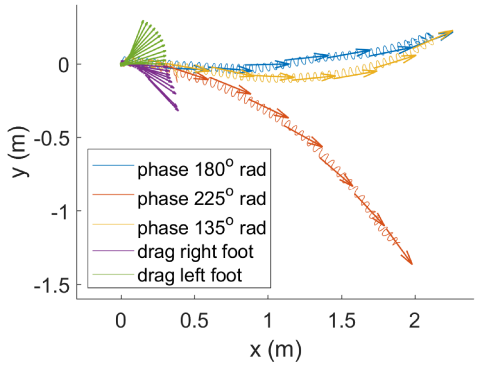

Fig. 8. Robot horizontal plane trajectories (position and heading) in turning trials using phase offset between the legs and foot dragging.

C. Horizontal Plane Testing

Yaw compensation has been a common problem for passive walkers with spherical feet. Several robots, such as those in [11] and [25], have implemented statically equivalent flat foot spring feet to increase ground contact and avoid unwanted yaw sway. Other solutions, such as in [24], include integrating counter swinging arms to provide counter torque to the unwanted yaw motion. Despite having spherical feet and no torso, we have been able to direct the heading of our robot by simply changing feed-forward control parameters.

Shown in Fig. 8, we attempted to control the heading of our walker by changing the sinusoidal phase offset shown in (2). From these initial results, we see that we can control the direction of our robot with a simple phase offset. These results show promise in being able to go straight or even control the heading of our robot if we were to implement feedback control. We also implemented a more extreme turn, also shown in Fig. 8, by fixing one leg at a short length rather than extending and retracting it, dragging that foot.

V. CONCLUSIONS

The quasi-passive walking model presented in this paper is quite simple: it has only a single actuator per leg, a total of 5 rigid bodies, and does not require any feedback control for a simple stable gait. Despite this simplicity, we are able to demonstrate three key features in simulation and experiments: 1) stable walking over a range of actuation parameters, 2) control over the heading, and 3) the ability to start and stop from a standing posture.

Our simulation and physical results show that feet with nonconcentric centers of curvature (unlike most prior walkers that used concentric feet, except for [23]) yield the most consistent walking. Additionally, we establish that the frequency of actuation and the forward velocity are inversely related above a minimal activation frequency.

Our goal with this project is to make miniature walking robots, as small as a Lego Minifigure [30] (1cm leg) or smaller, and this will be the focus of our future work. Due to the simplicity of actuation, lack of controller feedback, and scale-invariance of the model, it is feasible to shrink our robot down closer to that size. Through some initial prototyping, we have been able to shrink the walker to about 5cm leg length with electromagnetic actuation. By leveraging the model in this paper and integrating MEMS actuators, we believe a Lego sized bipedal walker is possible.

Through our simulation and physical testing, we have found some interesting relationships. For example, we see a likely relationship between walking consistency and gap width, in addition to the foot shape. While the negligible gap feet walk quickly in low amplitude physical experiments, they are somewhat less consistent than the other geometries. Consistent walking may be important for steadily maintaining heading and converging from disturbances. Further analysis of the energy effects, hybrid transitions, and dampening effects will likely be required to firmly establish this relationship. Additionally, we are excited by the prospect of being able to control the yaw of a bipedal walker with only two actuated degrees of freedom. Although we are able to turn the robot by changing the phase offset, it would be interesting to see if feedback control enables us to more precisely control the heading of the robot.

REFERENCES

[1] M. Bell, J. Weaver, and R. Wood, "An ambidextrous starfish-inspired exploration and reconnaissance robot (the ASTER-bot)," *Soft Robotics*, 12 2021.

[2] R. S. Pierre, D. Vogtmann, and S. Bergbreiter, "Model-based insights on the design of a hexapod magnetic walker," in *International Symposium on Experimental Robotics*, 2016, pp. 715–727.

[3] D. Kim, Z. Hao, J. Ueda, and A. Ansari, "A 5mg micro-bristle-bot fabricated by two-photon lithography," *Journal of Micromechanics and Microengineering*, vol. 29, 07 2019.

[4] K. Patel, J. Qu, and K. R. Oldham, "Tilted leg design for a rapid-prototyped low-voltage piezoelectric running robot," in *International Conference on Manipulation, Automation, and Robotics at Small Scales*, 2018, pp. 1–6.

[5] J. W. Grizzle, C. Chevallereau, R. W. Sinnet, and A. D. Ames, "Models, feedback control, and open problems of 3D bipedal robotic walking," *Automatica*, vol. 50, no. 8, pp. 1955–1988, 2014.

[6] T. McGeer, "Passive dynamic walking," *International Journal of Robotics Research*, vol. 9, no. 2, pp. 62–82, 1990.

[7] J. E. Wilson, "Walking toy," US Patent 2,140,275, Dec. 1938.

[8] R. Tedrake, T. Zhang, M. fai Fong, and H. Seung, "Actuating a simple 3D passive dynamic walker," *IEEE International Conference on Robotics and Automation*, vol. 5, pp. 4656–4661, 2004.

[9] S. Collins, A. Ruina, R. Tedrake, and M. Wisse, "Efficient bipedal robots based on passive-dynamic walkers," *Science*, vol. 307, no. 5712, pp. 1082–1085, 2005.

[10] P. A. Bhounsule, J. Cortell, A. Grewal *et al.*, "Low-bandwidth reflex-based control for lower power walking: 65 km on a single battery charge," *International Journal of Robotics Research*, vol. 33, no. 10, pp. 1305–1321, 2014.

[11] T. Kinugasa, K. Ando, S. Fujimoto *et al.*, "Development of a three-dimensional dynamic biped walking via the oscillation of telescopic knee joint and its gait analysis," *Journal of Mechanical Engineering and Sciences*, vol. 9, pp. 1529–1537, 12 2015.

[12] Y. Cao, S. Suzuki, Y. Hoshino *et al.*, "Gait stabilization of a quasi-passive walker based on energy balance by utilizing a mechanical oscillator," in *Asian Control Conference*, 2015, pp. 1–6.

[13] S. Murai, S. Fujimoto, A. Yamamoto, and T. Kinugasa, "3D quasi-passive walker of bipedal robot with flat feet gait analysis of 3D quasi-passive walking," in *International Conference on Multimedia Systems and Signal Processing*, 2016, pp. 74–79.

[14] A. M. Boudali, F. H. Kong, J. Martinez *et al.*, "Design and modeling of an open platform for dynamic walking research," in *IEEE International Conference on Mechatronics*, 2017, pp. 85–92.

[15] A. Goswami, B. Espiau, and A. Keramane, "Limit cycles in a passive compass gait biped and passivity-mimicking control laws," *Autonomous Robots*, vol. 4, no. 3, pp. 273–286, 1997.

[16] M. Garcia, A. Chatterjee, A. Ruina, and M. Coleman, "The simplest walking model: Stability, complexity, and scaling," *ASME Journal of Biomechanical Engineering*, 1998.

[17] S. Miyakoshi and G. Cheng, "Examining human walking characteristics with a telescopic compass-like biped walker model," in *IEEE International Conference on Systems, Man, and Cybernetics*, vol. 2, Nov. 2004, pp. 1538 – 1543.

[18] F. Asano and Z.-W. Luo, "Energy-efficient and high-speed dynamic biped locomotion based on principle of parametric excitation," *IEEE Transactions on Robotics*, vol. 24, no. 6, pp. 1289–1301, 2008.

[19] A. Kuo, "Energetics of actively powered locomotion using the simplest walking model." *Journal of Biomechanical Engineering*, vol. 124, no. 1, pp. 113–120, 2002.

[20] M. Zhao, H. Dong, and N. Zhang, "The instantaneous leg extension model of virtual slope walking," in *IEEE/RSJ International Conference on Intelligent Robots and Systems*, 2009, pp. 3220–3225.

[21] T. McGeer and L. H. Palmer, "Wobbling, toppling, and forces of contact," *American Journal of Physics*, vol. 57, no. 12, pp. 1089–1098, 1989.

[22] S. E. Sovero, C. O. Saglam, and K. Byl, "Passive frontal plane coupling in 3D walking," in *IEEE/RSJ International Conference on Intelligent Robots and Systems*, 2015, pp. 1605–1611.

[23] J. N. Martinez-Castelan and M. G. Villarreal-Cervantes, "Frontal-sagittal dynamic coupling in the optimal design of a passive bipedal walker," *IEEE Access*, vol. 7, pp. 427–449, 2018.

[24] S. Collins, M. Wisse, and A. Ruina, "A three-dimensional passive-dynamic walking robot with two legs and knees." *International Journal of Robotics Research*, vol. 20, pp. 607–615, 01 2001.

[25] K. Wang, P. Tobajas, J. Liu *et al.*, "Towards a 3D passive dynamic walker to study ankle and toe functions during walking motion," *Robotics and Autonomous Systems*, vol. 115, 02 2019.

[26] M. Karpelson, G.-Y. Wei, and R. J. Wood, "A review of actuation and power electronics options for flapping-wing robotic insects," in *2008 IEEE International Conference on Robotics and Automation*, 2008, pp. 779–786.

[27] B. Spletzer, "Scaling laws for mesoscale and microscale systems," Sandia National Labs., Tech. Rep., 1999.

[28] J. Pratt and G. Pratt, "Exploiting natural dynamics in the control of a 3D bipedal walking simulation," in *International Conference on Climbing and Walking Robots*, 1999.

[29] L. F. Shampine and M. W. Reichelt, "The MATLAB ODE suite," *SIAM Journal on Scientific Computing*, vol. 18, no. 1, pp. 1–22, 1997.

[30] G. K. Christiansen and J. N. Knudsen, "Toy figure," US Patent Des. 253,711, Dec. 1979.